**Cell Reports Methods, Volume *3***

## Supplemental information

# A microfluidics-enabled automated workflow of sample preparation for MS-based immunopeptidomics

**Xiaokang Li, Hui Song Pak, Florian Huber, Justine Michaux, Marie Taillandier-Coindard, Emma Ricart Altimiras, and Michal Bassani-Sternberg**

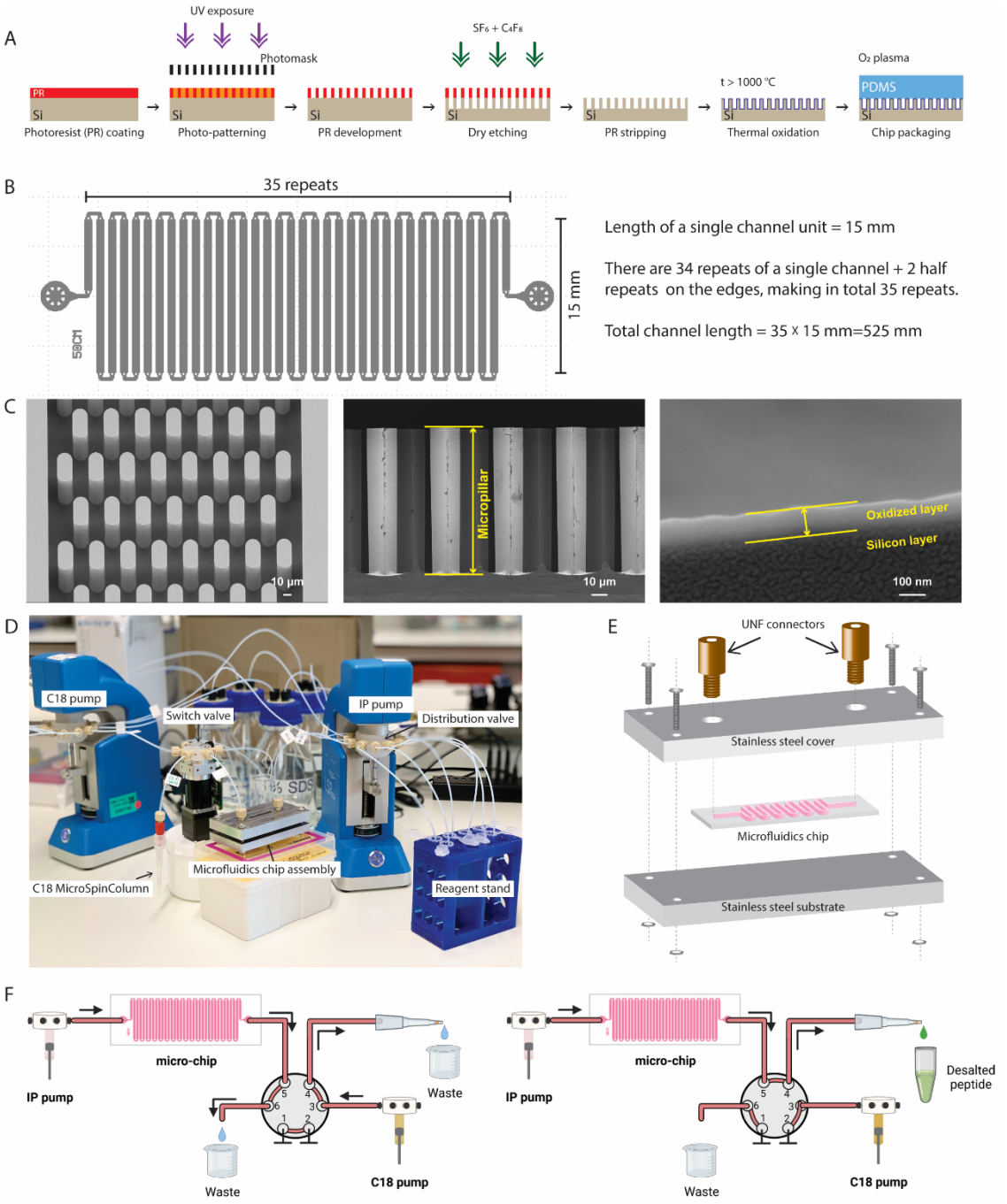


**Figure S1. Fabrication and the fluidic system setup of the microfluidics for chip-IP. Related to Figure 1.** (A) The schematic process of photolithography for fabricating the micropillar arrays on silicon substrate. (B) SEM characterization of the fluidic filters (left, scale bar = 10 µm), a cross-sectional view of the micropillars (middle, scale bar = 10 µm), and the oxidized silicon surface (right, scale bar = 100 nm). (C) A photograph showing the streamlined fluidic setup for the chip-IP and online C18 peptide cleanup. (D) An exploded-view drawing of the mechanical clamp for reinforcing the fluidic connections of chip-IP. (E) The flow diagram of a valve-enabled coupling between the chip-IP and the C18 cleanup steps (created with BioRender.com).

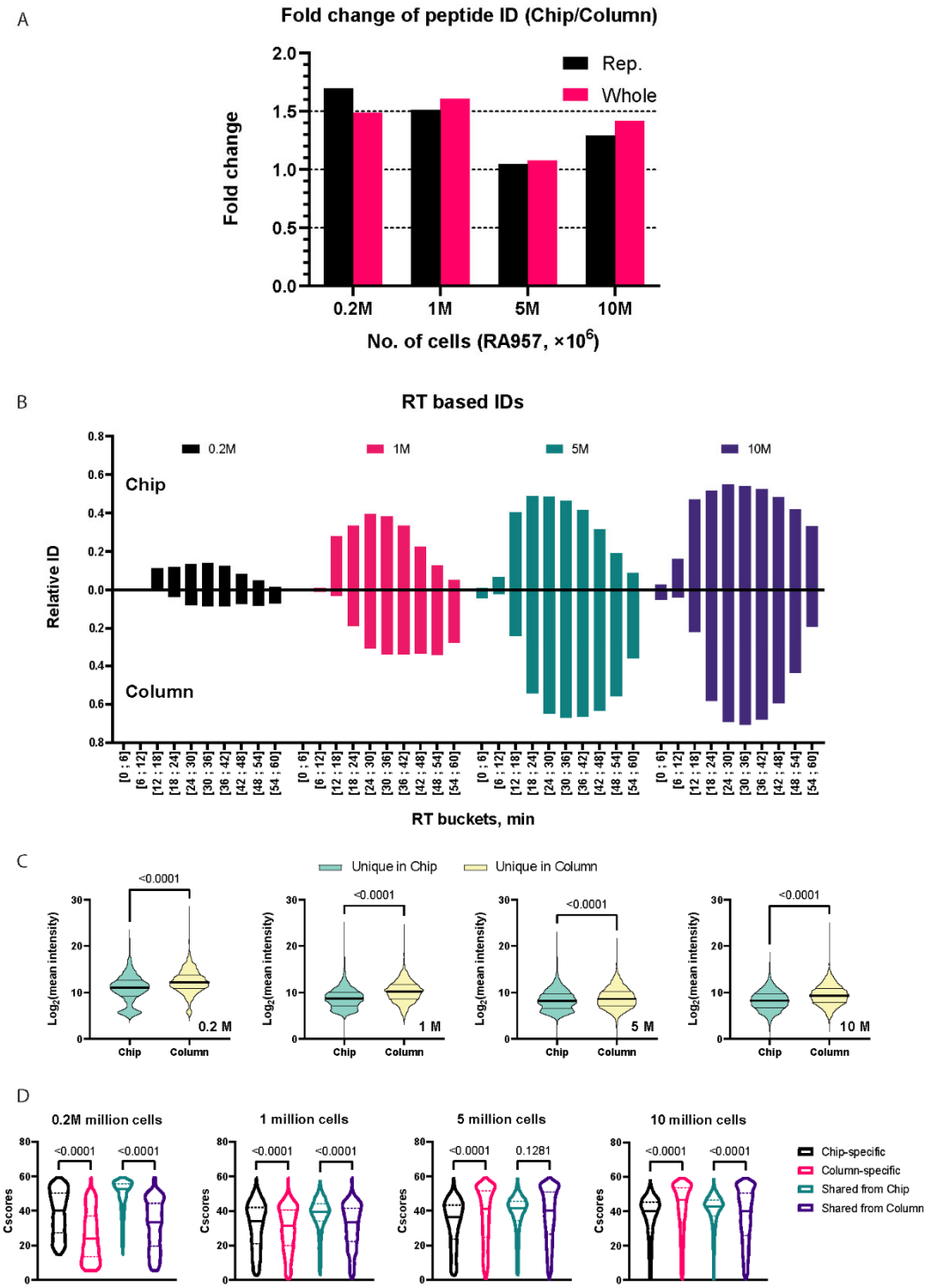


**Figure S2. Further comparisons of the identified peptides between the two IP methods. Related to Figure 2 and 3.** (A) The fold-change of peptide identification on the chip in relative to the column-IP. (B-C) Further comparisons of the peptide properties between chip- and column-IP. (B) A histogram showing the relative peptide identification in each cell group based on the peptides' retention times during the LC separation by the two methods. (C) The MS2 intensities of unique peptides depicted in violin plots. (D) Comparison of the identification scores (Cscore) for peptides enriched from different number of RA957 cells by Chip- and Column-IP. The Cscores were analyzed in violin plots for four categories of peptides identified in each cell group: chip-specific peptides, column-specific peptides, shared peptides with scores in the chip, and shared peptides with scores in the column. The solid lines in the plots indicate the median values while the dashes lines indicate the quartiles. The statistical analyses were performed by non-parametric one-way ANOVA tests.

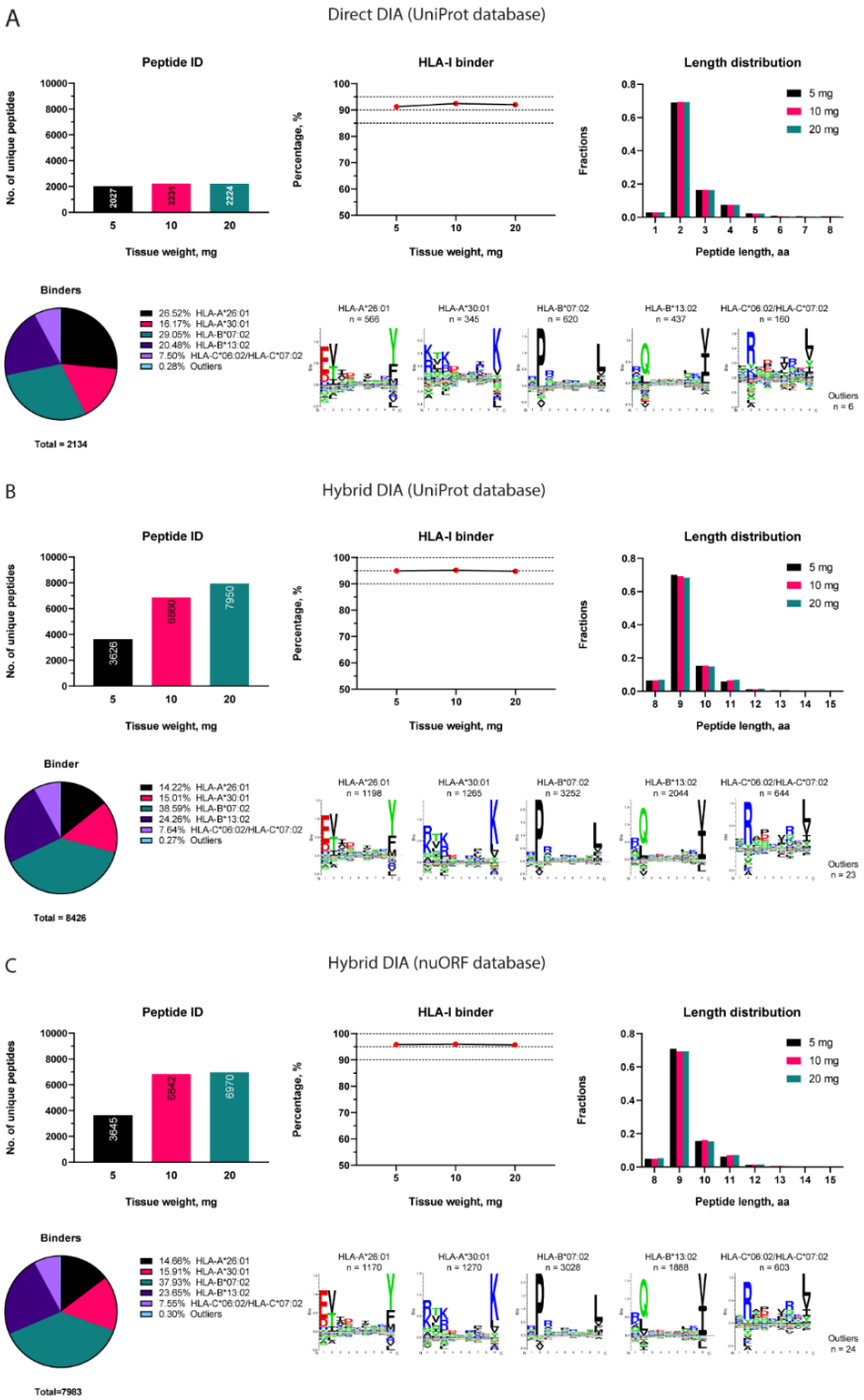


**Figure S3. Peptide identification from small liver metastasis tumor tissues by chip-IP. Related to STAR Methods.** The identification was performed by different approaches of DIA analysis: the library-free directDIA (A) and library-dependent hybridDIA (B-C). Some general aspects of the immunopeptidome were evaluated for each approach: The number of identified peptides, the percentage of HLA-I binders, the peptide length distribution, and the clustering of HLA-I binding motifs. The spectral library for hybridDIA analyses was built with DDA and DIA runs acquired from the small tissues (processed by chip-IP) as well as some bigger tissues sectioned from the same patient (processed by column-IP).

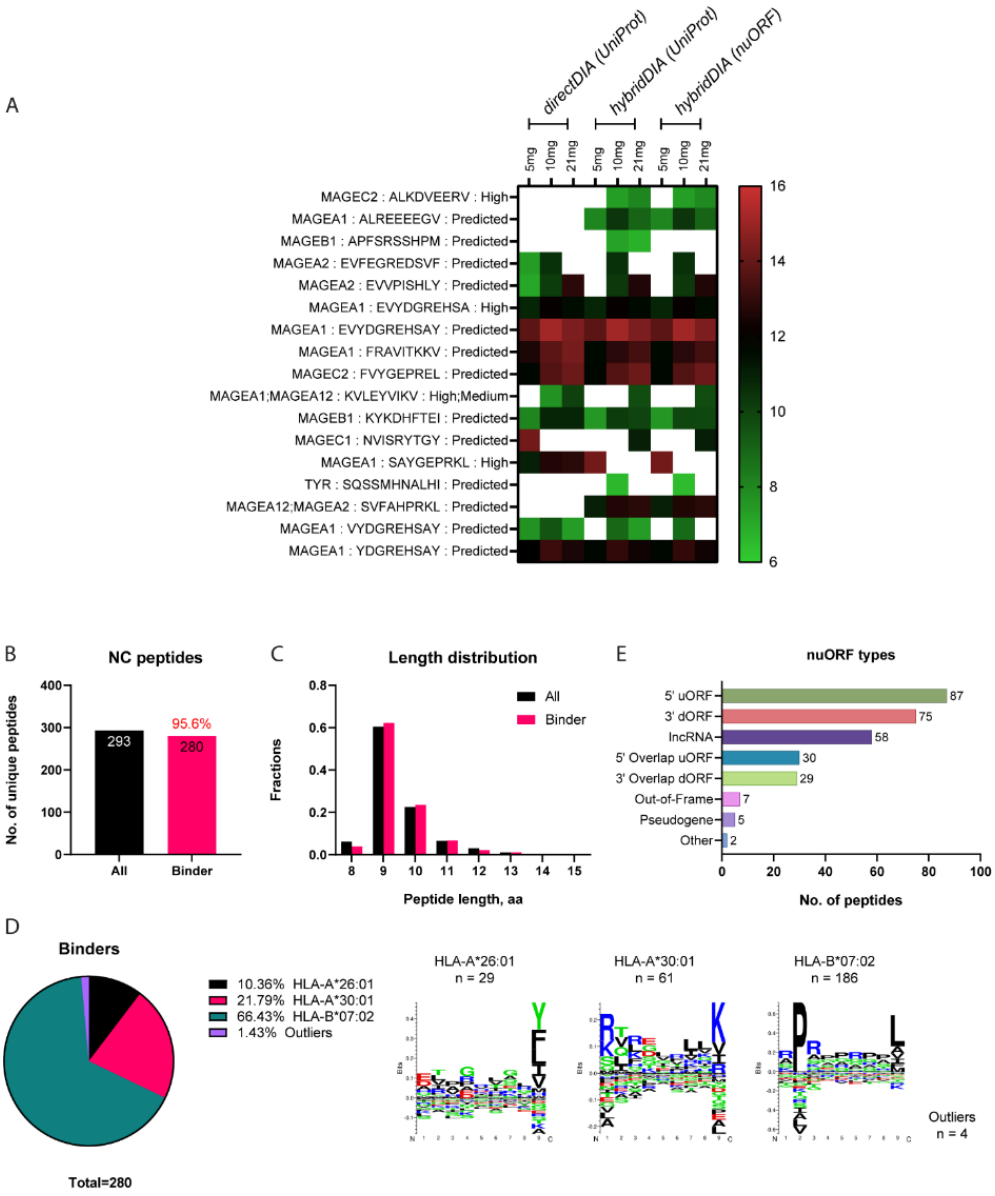


**Figure S4. The tumor-associated antigens (TAAs) and nuORF-derived antigens identified in the small liver metastasis tumor tissues by chip-IP. Related to STAR Methods.** (A) Identification of TAA peptides via chip-IP. The row titles were presented in the format of 'Gene name': 'Peptide sequence': 'Immunogenicity'. The immunogenicity level was labeled if it has been reported in relative literature, otherwise labeled as 'Predicted' if the peptide is derived from a typical TAA gene. Peptides 'ALKDVEERV', 'EVYDGREHSA', 'KVLEYVIKV', 'SAYGEPRKL' were tested immunogenic in references [1], [2], [3,4], [2,5], respectively. The enumeration of nuORF-derived peptides was shown in (B) where the percentage of predicted HLA-I binders was indicated in red. The length distribution and HLA-I motif clustering of nuORF peptides were shown in (C) and (D), respectively. (E) Types of nuORFs for the 293 non-canonical peptides.

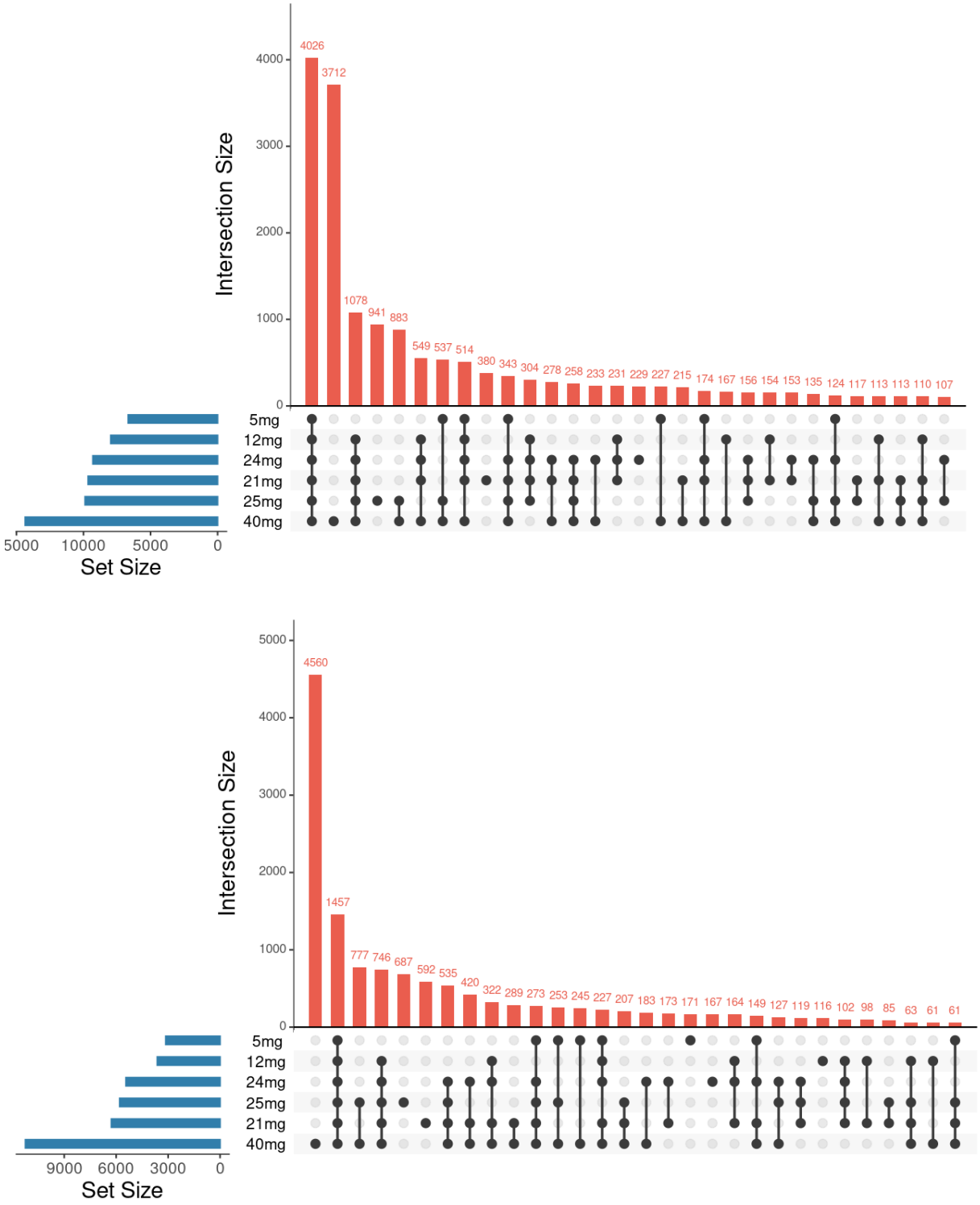


**Figure S5. The intersection of canonical peptide identification among the small malignant melanoma tissues. Related to Figure 4 and 6.** The UpSet plots were used to visualize the overlap of peptides for (Top) DIA analysis using the sample-specific spectral library and (Bottom) DIA analysis using the Lausanne-Lib. The UpSet plots were created with Intervene [6].

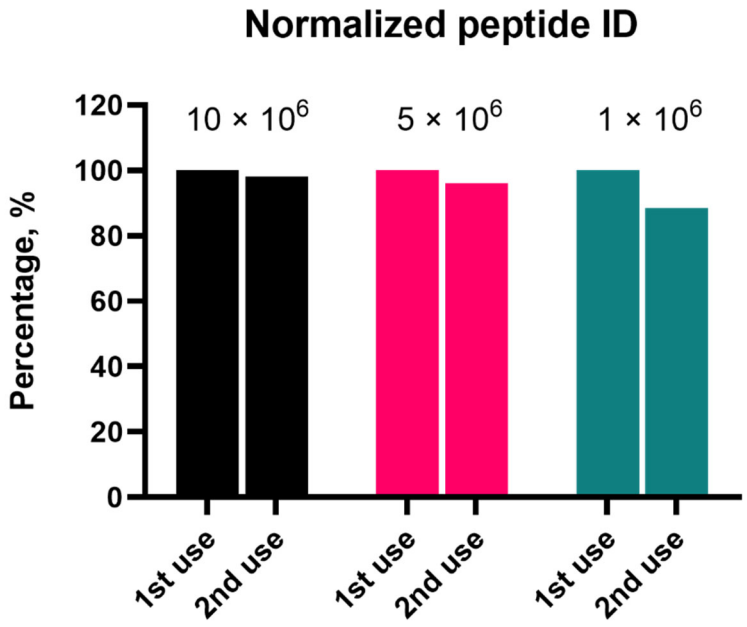


**Figure S6. The peptide identification from a preliminary test for chip reusability. Related to STAR Methods.** The test was done with three groups of RA957 cells (10 million, 5 million and 1 million) on three individual chips. The chips were washed with excessive acetic acid after the initial IP of each group. The resulting peptide identification was normalized to the bigger value in each group.

**Table S1. The flow chart for the chip functionalization, chip-IP and online C18 peptide cleanup. Related to STAR Methods.**

| Antibody coating and crosslinking | | | |
|---|---|---|---|
| **Step** | **Buffer** | **Volume (µL)** | **Flow rate (µL/min)** |
| Prime | Absolute ethanol | 200 | 20 |
| Silanization | 1 mM NHS-silane | 100 | NA (Static incubation for 2 hours) |
| Wash | Absolute ethanol | 200 | 10 |
| Coating 1 | 1 mg/mL Protein A/G | 100 | 5 |
| Wash | PBS, pH 7.2 | 200 | 20 |
| Coating 2 | 3 mg/mL pan-HLA antibody | 100 | 5 |
| Wash | PBS, pH 7.2 | 200 | 20 |
| Crosslink | 20mM DMP | 200 | 10 |
| Wash | PBS, pH 7.2 | 200 | 20 |
| Quench | 0.2M ethanolamine | 200 | 10 |
| Wash | PBS, pH 7.2 | 200 | 20 |
| Storage | 0.02% Na azide | 200 | 20 |
| **Chip-IP** | | | |
| **Step** | **Buffer** | **Volume (µL)** | **Flow rate (µL/min)** |
| Prime | 0.1N acetic acid | 200 | 20 |
| Equilibration | 0.1 Tris-HCl, pH 8 | 200 | 20 |
| Sample | Cell or tissue lysate | e.g., 100 | 5 |
| Wash 1 | Lysis buffer | 500 | 20 |
| Wash 2 | 0.02M Tris-HCl, pH 8 | 500 | 20 |
| Elution | 0.1N acetic acid | 250 | 10 (Elution flows directly into the preconditioned C18 materials) |
| Equilibration | 0.1 Tris-HCl, pH 8 | 200 | 20 |
| Storage | 0.02% Na azide | 200 | 20 |
| **Peptide cleanup (desalting)** | | | |
| **Step** | **Buffer** | **Volume (µL)** | **Flow rate (µL/min)** |
| Prime | 80% acetonitrile in 0.1% TFA | 250 | 2000 |
| Equilibration | 0.1% TFA | 500 | 2000 |
| Eluate loading | Acid elution from the on-chip IP | 250 | 10 |
| Wash | 0.1% TFA | 500 | 2000 |
| Peptide elution | 25% acetonitrile in 0.1% TFA | 250 | 2000 (Collect the peptides for vacuum drying) |

**Table S2. HLA typing information. Related to STAR Methods.**

| Samples | HLA-A | | HLA-B | | HLA-C | |
|---|---|---|---|---|---|---|
| RA 957 cells | A02:20 | A68:01 | B35:03 | B39:01 | C04:01 | C07:02 |
| Malignant melanoma patient | A01:01 | A03:01 | B08:01 | B57:01 | C06:02 | C07:01 |
| Liver metastasis of melanoma patient | A26:01 | A30:01 | B07:02 | B13:02 | C06:02 | C07:02 |

**References**


1. Ma, W., Germeau, C., Vigneron, N., Maernoudt, A.-S., Morel, S., Boon, T., Coulie, P.G., and Van den Eynde, B.J. (2004). Two new tumor-specific antigenic peptides encoded by gene MAGE-C2 and presented to cytolytic T lymphocytes by HLA-A2. Int. J. Cancer *109*, 698–702. 10.1002/ijc.20038.

2. Chaux, P., Luiten, R., Demotte, N., Vantomme, V., Stroobant, V., Traversari, C., Russo, V., Schultz, E., Cornelis, G.R., Boon, T., et al. (1999). Identification of five MAGE-A1 epitopes recognized by cytolytic T lymphocytes obtained by in vitro stimulation with dendritic cells transduced with MAGE-A1. J. Immunol. Baltim. Md 1950 *163*, 2928–2936.

3. Pascolo, S., Schirle, M., Gückel, B., Dumrese, T., Stumm, S., Kayser, S., Moris, A., Wallwiener, D., Rammensee, H.G., and Stevanovic, S. (2001). A MAGE-A1 HLA-A A*0201 epitope identified by mass spectrometry. Cancer Res. *61*, 4072–4077.

4. Ottaviani, S., Zhang, Y., Boon, T., and van der Bruggen, P. (2005). A MAGE-1 antigenic peptide recognized by human cytolytic T lymphocytes on HLA-A2 tumor cells. Cancer Immunol. Immunother. CII *54*, 1214–1220. 10.1007/s00262-005-0705-2.

5. van der Bruggen, P., Szikora, J.P., Boël, P., Wildmann, C., Somville, M., Sensi, M., and Boon, T. (1994). Autologous cytolytic T lymphocytes recognize a MAGE-1 nonapeptide on melanomas expressing HLA-Cw*1601. Eur. J. Immunol. *24*, 2134–2140. 10.1002/eji.1830240930.

6. Khan, A., and Mathelier, A. (2017). Intervene: a tool for intersection and visualization of multiple gene or genomic region sets. BMC Bioinformatics *18*, 287. 10.1186/s12859-017-1708-7.